Sensors and Actuators B 199 (2014) 361–368

Contents lists available at ScienceDirect

Sensors and Actuators B: Chemical

journal homepage: www.elsevier.com/locate/snb

Direct growth of titania nanotubes on plastic substrates and their application to flexible gas sensors

Nam-Su Jang [a], Min Seong Kim [b], Soo-Hyung Kim [a,b], Soo-Keun Lee [c,*], Jong-Man Kim [a,b,**]

[a] Department of Nano Fusion Technology, Pusan National University, Busan 609-735, Republic of Korea
[b] Department of Nanomechatronics Engineering, Pusan National University, Busan 609-735, Republic of Korea
[c] Nano & Bio Research Division, Daegu Gyeongbuk Institute of Science and Technology, Daegu 711-873, Republic of Korea

ARTICLE INFO

Article history:
Received 31 December 2013
Received in revised form 20 March 2014
Accepted 30 March 2014
Available online 18 April 2014

Keywords:
Titania nanotubes
Ti thin-film anodization
Plastic substrates
Flexible gas sensors

ABSTRACT

Titania nanotubes (TNTs) were directly synthesized on titanium thin-film deposited on plastic substrates by electrochemical anodization in ethylene glycol (EG)-based electrolyte containing ammonium fluoride (NH_4F) and water (H_2O). The effect of various anodization conditions such as growth time, H_2O content in electrolyte, anodization voltage, and electrolyte temperature on the morphologies of resultant TNTs was investigated. It was found that the addition of moderate amount of H_2O in electrolyte and subsequent HF treatment were beneficial to the formation of micrometer-long TNTs with open and regular tubular surfaces. After transition from amorphous to anatase phase by thermal annealing at 350 °C, the TNTs were employed as flexible chemoresistive sensors for detecting carbon monoxide (CO) and ammonia (NH_3) gases. The gas sensing performance of the flexible TNT sensors was characterized by measuring the changes in electrical current due to exposure to test gases and the corresponding gas responses. The sensor responses were considerably stable and reversible even under repetitive gas exposure at different concentrations. In addition, the gas responses were also found to be linear with respect to different concentrations of test gases and fairly good even at relatively low concentration.

1. Introduction

Over the past decade, highly-ordered titania nanotube (TNT) arrays have attracted great attention due to their large specific surface areas and superior catalytic reactivities, which are crucial to maximize the efficiency of titania-based semiconducting devices. Based on the unique physical and chemical properties of TNTs, their potential applications have been increasingly explored including gas sensors [1–5], dye-sensitized solar cells (DSSCs) [6–15], photocatalysts [16–20], electrochromic devices [21–25], humidity sensors [26,27], and so on. In recent years, many different approaches to synthesize TNTs have been investigated, such as sol–gel process [14,28,29], template-assisted atomic layer deposition (ALD) [19,30–32], hydrothermal method [15,20,33,34], and electrochemical anodization of titanium (Ti) [1–13,16–18,21–27]. Of these, anodization process has gained remarkable attention due to simple and cost-effective fabrication, and potential process scalability to large area. In addition, anodization approach enables to precisely control the morphologies (height, diameter, and wall thickness) of TNTs while retaining regular ordering by optimizing the process conditions such as electrolyte systems (aqueous and non-aqueous electrolytes) and anodization parameters (anodic voltage, anodization time, composition and temperature of electrolyte). More recently, as the growing demands for flexible electronics with new functionalities such as mechanical bendability, many researchers have tried to demonstrate TNT-based devices as flexible architectures to extend their potential applications. Several flexible applications have been demonstrated by anodizing Ti foils with the thickness of typically a few hundred micrometers [35–37]. Although this approach makes it possible to fabricate flexible TNTs with the help of flexible nature of Ti foils, their practical use would be limited by difficulty in integration with other circuits or systems through a batch-processing. Some researchers have developed a new class of TNT-based flexible devices by the electrochemical anodization of Ti meshes or wires instead of flat foils, resulting in improvement of the mechanical flexibility [38–40]. Nevertheless, this strategy still suffers from incompatibility with microfabrication technologies. In addition, more recently, highly-ordered TNT membranes, which are carefully detached from mother Ti foils after anodizing, have been transferred onto other flexible substrates [41]. However, this method includes some cumbersome processes such as detachment and

* Corresponding author.
** Corresponding author at: Department of Nano Fusion Technology, Pusan National University, Busan 609-735, Republic of Korea. Tel.: +82 553505288.
E-mail addresses: laser@dgist.ac.kr (S.-K. Lee), jongkim@pusan.ac.kr (J.-M. Kim).

http://dx.doi.org/10.1016/j.snb.2014.03.113
0925-4005/

manual assembly of freestanding TNT membranes, resulting in complex fabrication. In addition, low production yield would also be unavoidable in this approach due to the brittleness of TNT membranes. Therefore, it is of great technological interest to synthesize TNTs from Ti thin-films prepared on desired substrates in order to overcome the limitations of the bulky Ti foil-based approaches. For these reasons, many attempts are currently carrying out to grow TNTs directly from Ti films deposited on various functional substrates such as transparent glass [42,43], conducting glass [44–46], silicon [43,47], metal alloy [48], and alumina [43,49] by employing sputtering or evaporation techniques. Nevertheless, to date, there are few reports dealing with the parametric investigation of TNTs prepared directly on plastic substrates.

This paper reports parametric studies on the synthesis and morphologies of titania nanotube (TNT) arrays by electrochemical oxidation of Ti thin-film on plastic polyimide (PI) substrates under various anodization conditions for flexible applications. As a potential demonstration, gas sensing properties of the TNT-based flexible chemoresistive sensors are investigated.

2. Experiment details

2.1. Synthesis and characterization of TNT arrays on plastic substrate

In the present study, a polyimide (PI; Kapton 500 HN, Dupont) film with the thickness of ~125 μm was used as a flexible substrate because of its superior glass-transition temperature (T_g) as high as 360 °C. The high T_g of PI substrates is suitable for withstanding during the crystallization of TNTs at high temperature without appreciable degradation in the mechanical and chemical properties. ~2-μm-thick Ti film was deposited on a cleaned PI substrate by radio frequency (RF) magnetron sputtering under a working pressure of 5×10^{-3} Torr and sputtering power of 200 W. The substrate temperature was kept at 300 °C during sputtering process to improve both the density of the films and adhesion between the films and substrates. Highly ordered TNT arrays were synthesized through an electrochemical anodization of Ti films prepared on PI substrates with a fixed area of 1.5 cm × 1 cm in a two-electrode system. A platinum (Pt)-coated Ti plate with an area of 5 cm × 6 cm was employed as a counter electrode. During anodization, the distance between the sample and counter electrode was constantly kept at 3 cm. The prepared electrolyte was stirred magnetically for 1 h prior to all the anodization experiments.

The anodization process was conducted in a bath containing 0.75 wt% NH_4F and H_2O (2–10 vol%) in ethylene glycol (EG) solution (total volume of electrolyte: ~200 mL) for 10–30 min. The anodic potential (20–60 V) was applied using a DC power supply (Xantrex, XFR 600-2) in a potentiostatic mode with an increase rate of ~1 V/s. The temperature (5–40 °C) of electrolyte solution was precisely controlled during the anodization by a high/low-temperature bath circulator (JEIO TECH, RW-1025G). All the samples anodized under various conditions were further cleaned through a sonication process in a bath containing 0.05 wt% HF solution for 5 min to obtain open and regular nanotubular surfaces (hereafter, this cleaning process is referred to as the HF treatment). Finally, the prepared TNTs were thermally annealed at 350 °C in ambient air for 3 h in order to transform the as-anodized amorphous TNTs into the anatase crystal phase.

For the morphological characterization of the prepared TNTs, field emission scanning electron microscope (FESEM; HITACHI, S4700) was employed. High magnification morphologies and structures were investigated using transmission electron microscopy (TEM; JEOL, JEM 2100F), high resolution TEM (HRTEM), and selected area electron diffraction (SAED). The phase transition due to post-annealing was analyzed by X-ray diffraction (XRD; PANalytical, Empyrean Series 2) with CuK_α radiation.

A mechanical bending test of the TNTs prepared on PI substrates was performed under deformation at various bending radii after integrating them onto a home-made manual jig while monitoring the resultant electrical resistance of TNTs using a digital multimeter.

2.2. Fabrication and characterization of TNT-based flexible gas sensor

TNT-based flexible gas sensors were demonstrated by forming interdigitated sensing electrodes on TNT arrays prepared on PI substrate through standard microfabrication technologies. In detail, a 1.4-μm-thick photoresist (PR; Clariant, AZ5214) mold with a negative sidewall profile was first patterned on the TNT arrays. The interdigitated electrodes were then produced by the deposition of a 150-nm-thick aluminum (Al) layer using a thermal evaporation technique, followed by a lift-off process in an ultrasonic bath containing acetone.

The sensing properties of the fabricated TNT-based flexible gas sensors were investigated by characterizing the electrical properties of TNTs in response to different test gases such as CO and NH_3 under vacuum. For the measurements, 20% oxygen (O_2) in nitrogen (N_2) was employed as a carrier gas to simulate normal air conditions, and high-purity (>99.999%) test gases were supplied from gas cylinders with a concentration of 1000 ppm. The concentrations of the carrier and test gases injected to sensing chamber were precisely controlled by distinct mass-flow controllers (MFCs) connected to a computer equipped with Labview interfaces. Subsequently, the gases were mixed with a gas-mixer before introducing to the sensing chamber. During the measurement, the temperature in the sensing chamber was uniformly retained at 350 °C with a heating stage connected to a temperature control module. The changes in the electrical current of the sensors due to gas exposure were measured by a parameter analyzer (4200-SCS, Keithley). The gas response of the sensors was evaluated by the percentile electrical current change when the devices were exposed to gas molecules.

3. Results and discussion

3.1. Morphological studies of TNTs on plastic substrate

Fig. 1(a)–(c) shows the surface morphologies of TNTs anodized in 0.75 wt% NH_4F/EG electrolyte containing 2 vol% H_2O under anodization voltage of 40 V and electrolyte temperature of 25 °C for 10, 20, and 30 min, respectively. The resultant heights of TNTs are plotted in Fig. 1(d) with insets of the corresponding cross-sectional SEM images. Although the heights of TNTs were linearly increased as increasing the anodization time of up to 30 min, tubular structures were not seen on the surfaces of the anodized samples, as shown in Fig. 1(a)–(c). Moreover, surface morphologies of the samples were not significantly changed regardless of the post HF treatment. This means that compact oxide layer established in the early stages of the anodization process is quite strongly attached to TNTs, while entirely covering them. In general, the compact oxide layer can fully be dissolved by considerably increasing the anodization time [46]. However, a long synthesis time is not adequate for the anodization of Ti thin-film, because initial thickness of the sputter-deposited Ti is limited typically to a few micrometers. Moreover, the over-anodization might result in detachment of TNTs from the substrate by excessively consuming the underlying Ti film. Therefore, the anodization conditions must be carefully optimized to obtain clean tubular surface morphologies of TNTs

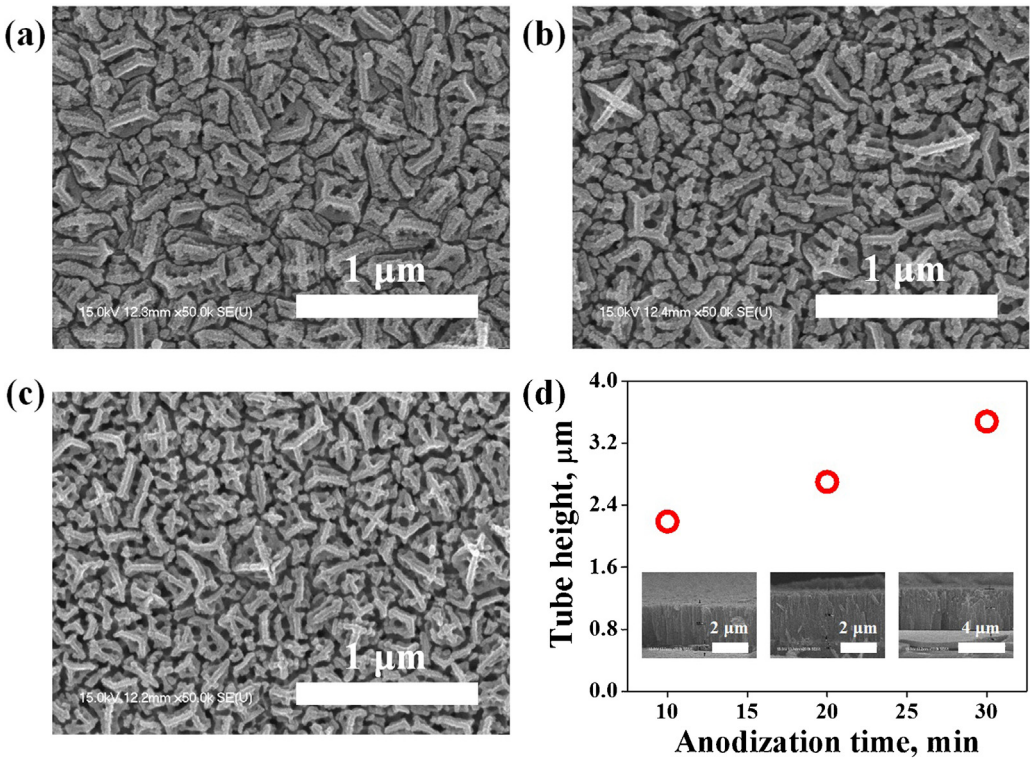

Fig. 1. Morphologies of TNTs anodized in 0.75 wt% NH_4F/EG electrolyte containing 2 vol% H_2O under anodization voltage of 40 V and electrolyte temperature of 25 °C for different anodization times (after HF treatment). (a)–(c) SEM images of surface morphologies of TNTs anodized for 10, 20, and 30 min, respectively, and (d) the heights of TNTs as a function of anodization time (inset: cross-sectional SEM images of each sample).

during anodization of Ti thin-films on plastic substrates for their potential flexible applications.

Increase of H_2O contents in electrolyte can be one of the easiest approaches to remove the compact oxide layer by accelerating the chemical dissolution of the oxide. Fig. 2(a) shows the SEM images of surface morphologies of TNTs prepared in electrolyte with the increased H_2O content (10 vol%) and subsequently sonicated in diluted HF solution. The insets of Fig. 2(a) show the corresponding surface morphologies of TNTs before the HF treatment. Although the porous surface morphologies of TNTs became apparent after the HF treatment, tubular structures did not appear on the surface with the anodization time of up to 20 min. However, many portions of the compact oxide layer were chemically dissolved during the anodization for 30 min, partially revealing the underlying regular TNTs. After the subsequent HF treatment, perfectly clean tubular surfaces of TNTs appeared, as shown in Fig. 2(a). This suggests that sufficient reaction time is still required for the preparation of clean tubular morphologies of TNTs even when the H_2O content in electrolyte was increased. However, the heights of TNTs were gradually decreased with the increased H_2O contents, as shown in Fig. 2(b). This mainly originates from the fact that the higher H_2O contents result in the faster dissolution of the oxide by a local acidification at the pore bottom due to the increase of H^+ ions in electrolyte. In this context, further increase of H_2O contents is undesirable for the practical applications that require the large specific surface area. Fig. 2(c) shows the heights of TNTs anodized in electrolyte containing 10 vol% H_2O, indicating the linear relationship with respect to the anodization time. In particular, the heights of TNTs were retained without significant changes even after the HF treatment. This suggests that the combination of moderate amount of H_2O addition and subsequent HF treatment is effective in obtaining micrometer-long TNTs with clean surface morphologies.

The anodization voltage and electrolyte temperature are also important influential factors for tailoring the rates of field-assisted oxidation and chemical (and field-assisted) dissolution, resulting in control of TNT architectures. Fig. 3 shows the morphological changes of TNTs anodized in 0.75 wt% NH_4F/EG electrolyte containing 10 vol% H_2O under different anodization voltages (20, 40, 60 V) and electrolyte temperatures (5, 25, 40 °C) for 30 min. The insets of Fig. 3 show the SEM images of cross-sections and surface morphologies of each sample. As shown in Fig. 3, the heights and inner diameters of TNTs were increased as increasing the anodization voltage and electrolyte temperature, indicating similar tendency. The surfaces of TNTs were partially and entirely covered with compact initial oxide layer even after the HF treatment under anodization voltage of 20 V and electrolyte temperature of 5 °C. This means that the electrochemical reactions are insufficient for obtaining clear morphologies in these anodization conditions. At the elevated anodization voltage and electrolyte temperature, the heights and inner diameters of TNTs were accordingly increased, revealing clear tubular structures. Interestingly, increase rates of the inner diameters were found be higher than those of the heights in both cases applying the elevated conditions, as shown in Fig. 3. This might be due to greatly enhanced chemical and field-assisted dissolution of the oxide compared to promotion of electrochemical oxidation of Ti film under the elevated conditions. First, the mobility of F^- ions in electrolyte would be more increased due to decrease in viscosity of electrolyte at elevated temperature, resulting in faster chemical dissolution of the oxide. In addition, increase in electric field intensity at higher anodization voltage would lead to a significant acceleration of field-assisted dissolution of the oxide. In this case, it should be noted that the specific surface areas can be decreased both under anodization voltage of 60 V and electrolyte temperature of 40 °C. This would be probably due to decrease in the number of TNTs in equivalent area, because pore diameters of TNTs are more rapidly increased, although the heights are also increased at the elevated conditions [9].

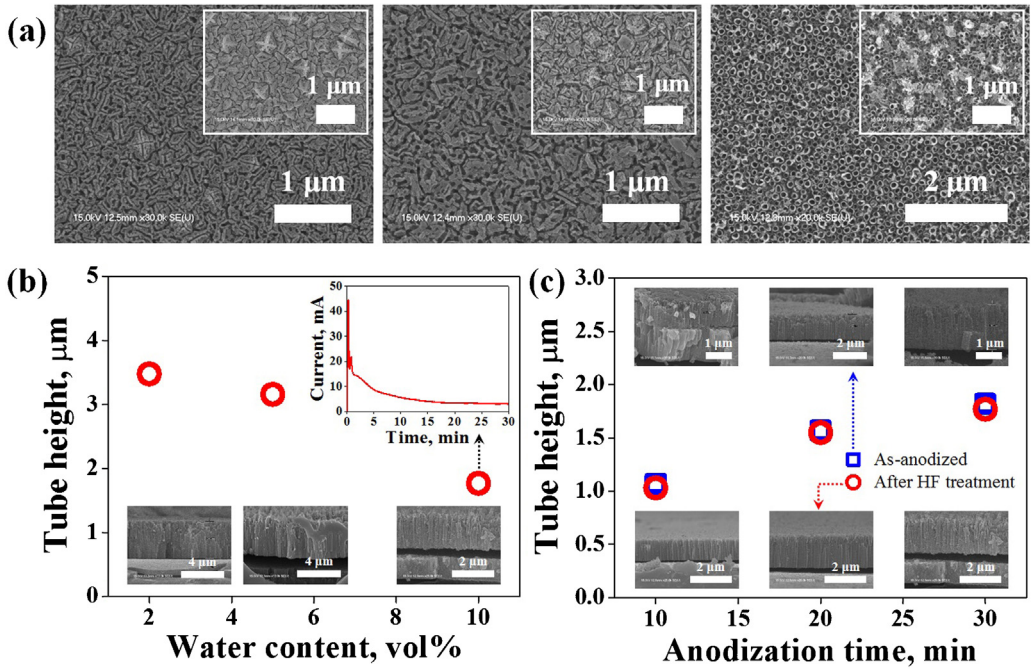

Fig. 2. (a) SEM images of surface morphologies of TNTs anodized in 0.75 wt% NH_4F/EG electrolyte containing 10 vol% H_2O under anodization voltage of 40 V and electrolyte temperature of 25 °C for different anodization times (after HF treatment) (insets: SEM images of TNTs before HF treatment), (b) the heights of TNTs as a function of H_2O content (insets: cross-sectional SEM images of each sample and typical current-time characteristics during anodization process (10 vol% H_2O)), and (c) the heights of TNTs before and after the HF treatment as a function of anodization time (insets: cross-sectional SEM images of each sample).

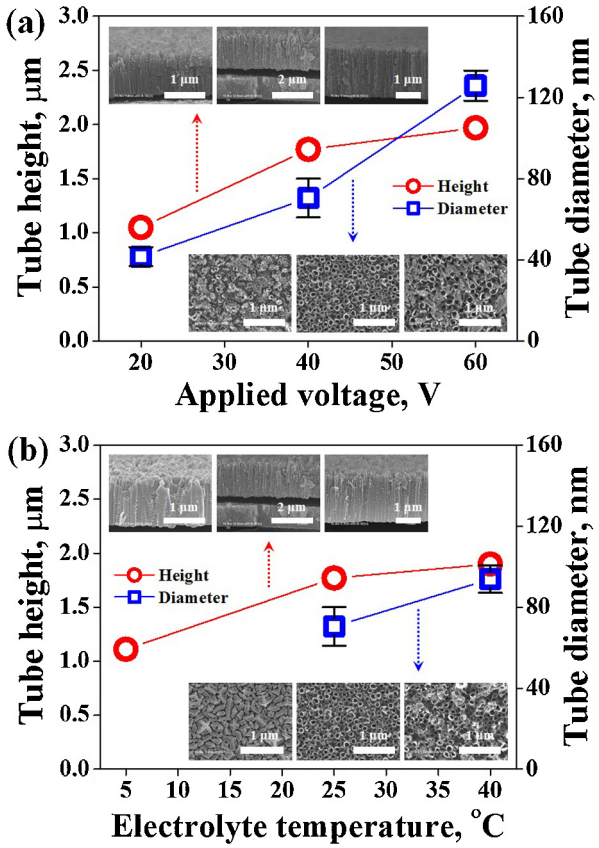

Fig. 3. Morphologies of TNTs anodized in 0.75 wt% NH_4F/EG electrolyte containing 10 vol% H_2O under different anodization voltages and electrolyte temperatures for 30 min (after HF treatment) (insets: SEM images of cross-sections and surface morphologies of each sample). (a) Under different anodization voltages of 20, 40, and 60 V and (b) under different electrolyte temperatures of 5, 25, and 40 °C.

Fig. 4 shows high magnification morphologies and structures of TNTs anodized in 0.75 wt% NH_4F/EG electrolyte containing 10 vol% H_2O under anodization voltage of 40 V and electrolyte temperature of 25 °C for 30 min. TEM image in Fig. 4(a) clearly represents highly ordered tubular structures of the prepared TNTs with quite uniform morphologies. Fig. 4(b) shows HRTEM image taken from the nanotube wall. The lattice spacing was observed to ~0.35 nm, which corresponds to (1 0 1) crystal plane of titania anatase phase. The corresponding SAED patterns also clearly confirm the crystalline structure of the TNTs, as shown in the inset in Fig. 4(b). Fig. 5 shows the XRD spectra of as-anodized and annealed TNTs. The XRD pattern of the as-anodized TNTs indicates amorphous structures with no crystalline phases. However, the highest peak that agreed with anatase phase (2θ = ~25.4°) corresponding to (1 0 1) crystal orientation clearly appeared in the XRD pattern of the TNTs annealed at 350 °C, which is consistent with the results of HRTEM and SAED investigations (Fig. 4(b)). This suggests that the as-anodized TNTs can be successfully crystallized to anatase phase at 350 °C without significant degradation in intrinsic properties of the PI substrates with T_g higher than 360 °C.

Fig. 6 shows the normalized resistance (R/R_0) of TNTs as a function of bending radius. The initial resistance (R_0) measured without imposing bending deformation was ~1.4 MΩ. The electrical resistance of TNTs was retained without appreciable degradation up to a minimum bending radius of ~2 mm, as shown in Fig. 6. The inset in Fig. 6 shows the R/R_0 of TNTs according to cyclic bending with a minimum bending radius of 6 mm, indicating no electrical failure even repetitive bending deformation of up to 20 cycles. These indicate that the TNTs prepared on plastic PI substrates are mechanically stable enough to be employed in flexible applications.

3.2. *Gas sensing properties of TiO_2 nanotube-based flexible gas sensor*

Fig. 7(a) shows the schematic illustrations of fabrication procedures of the proposed TNT-based flexible gas sensors (see Section

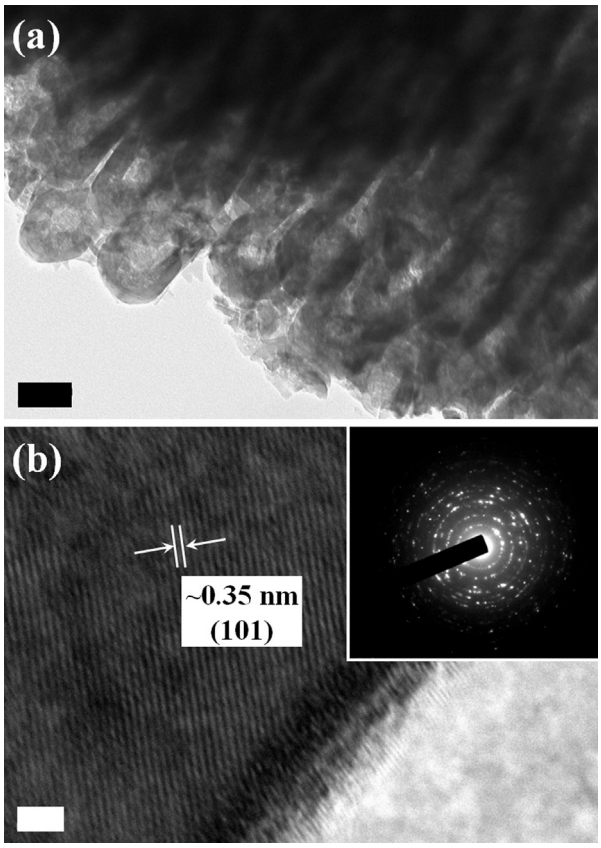

Fig. 4. High magnification morphologies and structures of TNTs anodized in 0.75 wt% NH_4F/EG electrolyte containing 10 vol% H_2O under anodization voltage of 40 V and electrolyte temperature of 25 °C for 30 min (after HF treatment). (a) TEM image (scale bar: 100 nm), and (b) HRTEM image (scale bar: 2 nm) (inset: SAED patterns).

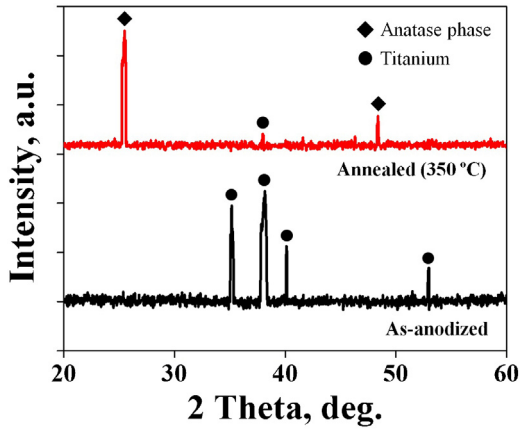

Fig. 5. XRD spectra for as-anodized and annealed (350 °C) TNTs.

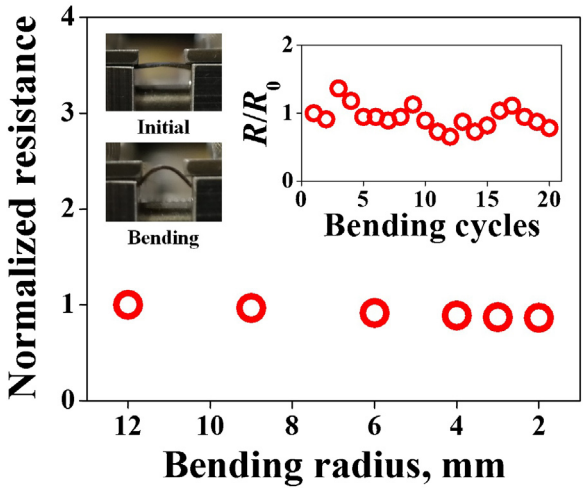

Fig. 6. Normalized electrical resistance (R/R_0) of TNTs as a function of bending radius during mechanical bending test (insets: digital images of TNTs at initial and bending states (left), R/R_0 of TNTs as a function of repetitive bending deformation of up to 20 cycles with a minimum bending radius of 6 mm (right)).

2). In this case, TNTs were prepared by the anodization process in 0.75 wt% NH_4F/EG electrolyte containing 10 vol% H_2O under anodization voltage of 40 V and electrolyte temperature of 25 °C for 30 min. The mechanical flexibility of the fabricated gas sensor was clearly demonstrated in Fig. 7(b).

Fig. 8(a) shows a simplified schematic illustraion of gas sensing system used in this work. The gas sensing properties of the fabricated flexible TNT devices were represented as normalized current, which indicates the ratio of the electrical current (I_{gas}) after exposure to test gases to that (I_0) in the initial state. In this case, the initial state means that the sensing chamber is filled with the carrier gas with the absence of the test gases. All the gas measurements were carried out at 350 °C. Fig. 8(b) and (c) shows the normalized current (I_{gas}/I_0) measured with different concentrations (50–200 ppm) of CO and NH_3 gases, respectively. These results

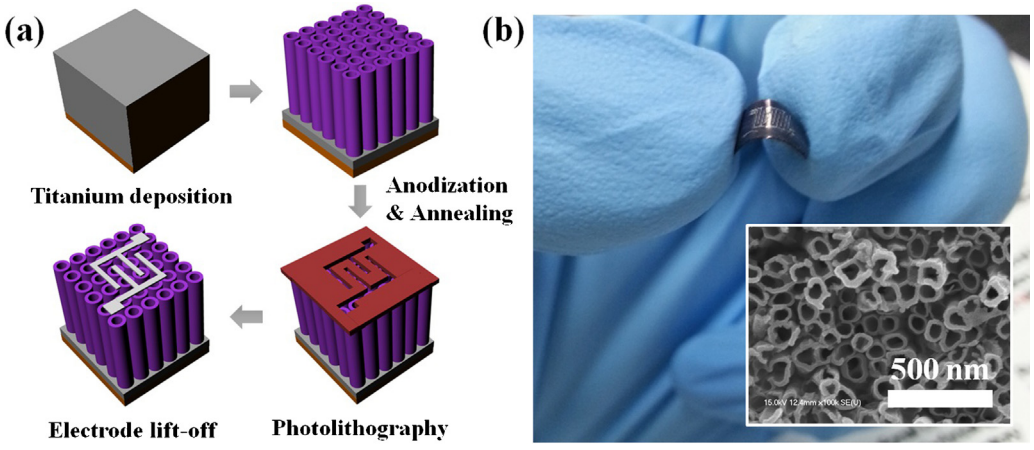

Fig. 7. Fabrication of TNT-based flexible gas sensors. (a) schematic illustrations of fabrication process and (b) digital image of the fabricated TNT-based flexible gas sensor.

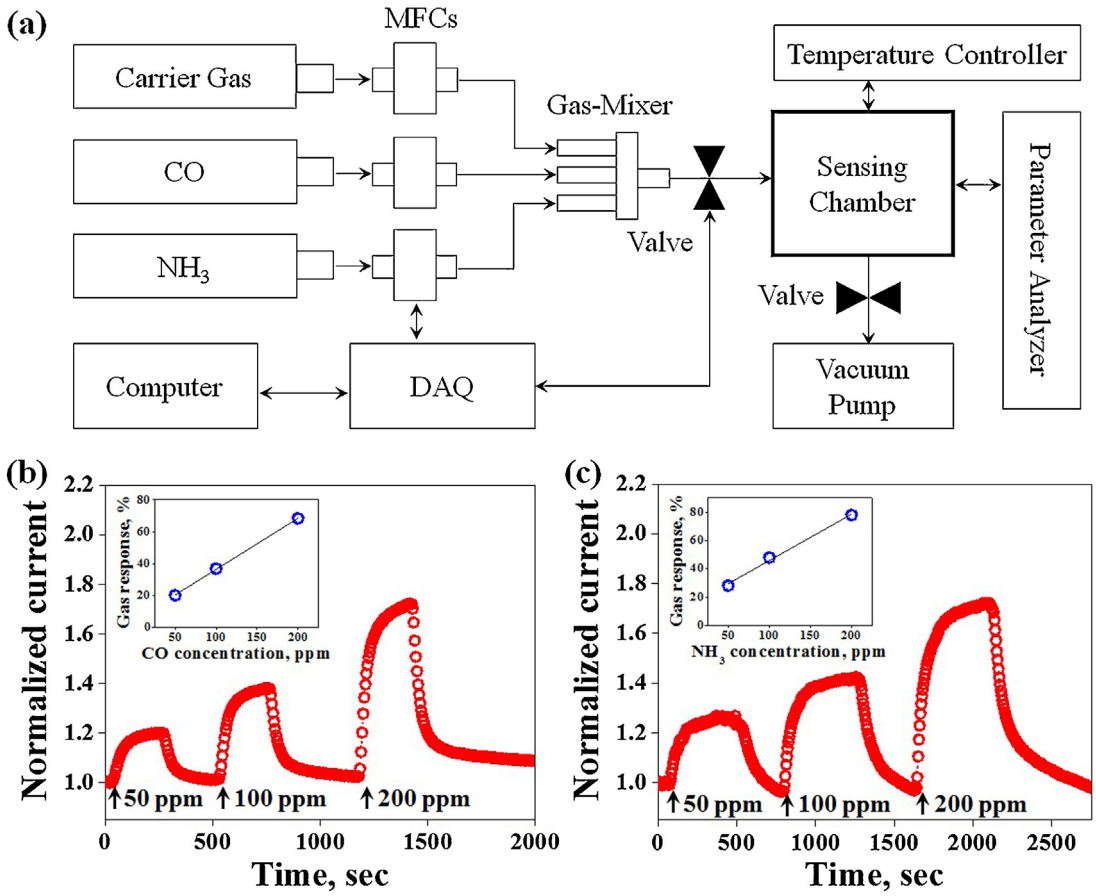

Fig. 8. Gas sensing properties of TNT-based flexible gas sensors under a working temperature of 350 °C. (a) Simplified schematic illustration of gas sensing system, (b) normalized current as a function of CO concentrations (inset: gas response to CO at different concentrations), and (c) normalized current as a function of NH_3 concentrations (inset: gas response to NH_3 at different concentrations).

suggest that the sensor responses were quite stable and reversible even under repetitive exposure to the test gases with different concentrations. In addition, it was clearly shown that the sensor responses were considerably fast, showing the response time of less than 1 min for 200 ppm of test gases. In this case, the response time was defined as the time needed to reach 50% of the maximum current change after exposure to test gases. The sensing performance of the flexible TNT sensors was evaluated by the gas response that defined as $(I_{gas} - I_0)/I_0 \times 100$ (%). The insets of Fig. 8(b) and (c) depict the gas responses of the devices for CO and NH_3 gases, respectively. A linear increase in gas responses was clearly observed at relatively low gas concentrations, and fairly good gas responses (68.3% and 77.9% for 200 ppm of CO and NH_3 gases, respectively) were achieved.

In principle, TNTs can be used to detect many different gases. In this regard, the approach described in this work provides the possibility for the development of versatile TNT-based gas sensors in flexible platforms.

4. Conclusion

In summary, highly-ordered micrometer-long TNTs with clean surface morphologies were successfully prepared on plastic substrates by the electrochemical anodization process. The surface morphologies of TNTs due to variations in anodization conditions such as synthesis time, H_2O content in electrolyte, anodic voltage, and electrolyte temperature, were investigated. The combination of moderate amount of H_2O addition and subsequent HF treatment (with mild sonication) is very helpful for obtaining clear and regular tubular structures of TNTs. The as-anodized TNTs were successfully crystallized to anatase phase at 350 °C without appreciable degradation in mechanical and chemical properties of the PI substrates.

As a potential application, flexible gas sensors based on TNTs with the height of ~1.8 μm and inner pore diameter of 70.5 ± 9.5 nm were fabricated by patterning the interdigitated sensing electrode though photolithography and lift-off processes. The sensor responses were considerably stable and reversible under repetitive exposure to CO and NH_3 gases at different concentrations. In addition, the gas responses were quite linear with respect to different concentrations of test gases and fairly good for 200 ppm of CO (68.3%) and NH_3 (77.9%) gases. Direct synthesis and morphological optimization of TNTs on plastic substrates are promising for the development of TNT-based flexible devices such as chemical sensors and dye-sensitized solar cells (DSSCs).

Acknowledgement

This research was supported by the Civil & Military Technology Cooperation Program through the National Research Foundation of Korea (NRF) funded by Ministry of Science, ICT & Future Planning (No. 2013M3C1A9055407).

References

[1] H.F. Lu, F. Li, G. Liu, Z.-G. Chen, D.-W. Wang, H.-T. Fang, G.Q. Lu, Z.H. Jiang, H.-M. Cheng, Amorphous TiO_2 nanotube arrays for low-temperature oxygen sensors, Nanotechnology 19 (2008) 405504.

[2] O.K. Varghese, D. Gong, M. Paulose, K.G. Ong, C.A. Grimes, Hydrogen sensing using titania nanotubes, Sens. Actuators B: Chem. 93 (2003) 338–344.
[3] E. Şennik, Z. Çolak, N. Kılınc, Z.Z. Öztürk, Synthesis of highly-ordered TiO_2 nanotubes for a hydrogen sensor, Int. J. Hydrog. Energy 35 (2010) 4420–4427.
[4] P.M. Perillo, D.F. Rodríguez, The gas sensing properties at room temperature of TiO_2 nanotubes by anodization, Sens. Actuators B: Chem. 171–172 (2012) 639–643.
[5] G.K. Mor, M.A. Carvalho, O.K. Varghese, M.V. Pishko, C.A. Grimes, A room-temperature TiO_2-nanotube hydrogen sensor able to self-clean photoactively from environmental contamination, J. Mater. Res. 19 (2004) 628–634.
[6] M. Ye, X. Xin, C. Lin, Z. Lin, High efficiency dye-sensitized solar cells based on hierarchically structured nanotubes, Nano Lett. 11 (2011) 3214–3220.
[7] J. Lin, J. Chen, X. Chen, High-efficiency dye-sensitized solar cells based on robust and both-end-open TiO_2 nanotube membranes, Nanoscale Res. Lett. 6 (2011) 475.
[8] K. Lee, D. Kim, P. Schmuki, Highly self-ordered nanochannel TiO_2 structures by anodization in a hot glycerol electrolyte, Chem. Commun. 47 (2011) 5789–5791.
[9] K. Shankar, G.K. Mor, H.E. Prakasam, S. Yoriya, M. Paulose, O.K. Varghese, C.A. Grimes, Highly-ordered TiO_2 nanotube arrays up to 220 μm in length: use in water photoelectrolysis and dye-sensitized solar cells, Nanotechnology 18 (2007) 065707.
[10] Q. Chen, D. Xu, Large-scale, noncurling, and free-standing crystallized TiO_2 nanotube arrays for dye-sensitized solar cells, J. Phys. Chem. C 113 (2009) 6310–6314.
[11] C.-J. Lin, W.-Y. Yu, S.-H. Chien, Transparent electrodes of ordered opened-end TiO_2-nanotube arrays for highly efficient dye-sensitized solar cells, J. Mater. Chem. 20 (2010) 1073–1077.
[12] Q. Pang, L. Leng, L. Zhao, L. Zhou, C. Liang, Y. Lan, Dye sensitized solar cells using freestanding TiO_2 nanotube arrays on FTO substrate as photoanode, Mater. Chem. Phys. 125 (2011) 612–616.
[13] J.H. Park, T.-W. Lee, M.G. Kang, Growth, detachment and transfer of highly-ordered TiO_2 nanotube arrays: use in dye-sensitized solar cells, Chem. Commun. (2008) 2867–2869.
[14] T.-S. Kang, A.P. Smith, B.E. Taylor, M.F. Durstock, Fabrication of highly-ordered TiO_2 nanotube arrays and their use in dye-sensitized solar cells, Nano Lett. 9 (2009) 601–606.
[15] M. Myahkostupov, M. Zamkov, F.N. Castellano, Dye-sensitized photovoltaic properties of hydrothermally prepared TiO_2 nanotubes, Energy Environ. Sci. 4 (2011) 998–1010.
[16] S.P. Albu, A. Ghicov, J.M. Macak, R. Hahn, P. Schmuki, Self-organized, free-standing TiO_2 nanotube membrane for flow-through photocatalytic applications, Nano Lett. 7 (2007) 1286–1289.
[17] J.M. Macak, M. Zlamal, J. Krysa, P. Schmuki, Self organized TiO_2 nanotube layers as highly efficient photocatalysts, Small 3 (2007) 300–304.
[18] C.-J. Lin, W.-Y. Yu, Y.-T. Lu, S.-H. Chien, Fabrication of open-ended high aspect-ratio anodic TiO_2 nanotube films for photocatalytic and photoelectrocatalytic applications, Chem. Commun. (2008) 6031–6033.
[19] W.-T. Chang, Y.-C. Hsueh, S.-H. Huang, K.-I. Liu, C.-C. Kei, T.-P. Perng, Fabrication of Ag-loaded multi-walled TiO_2 nanotube arrays and their photocatalytic activity, J. Mater. Chem. A 1 (2013) 1987–1991.
[20] S. Xu, J. Ng, A.J. Du, J. Liu, D.D. Sun, Highly efficient TiO_2 nanotube photocatalyst for simultaneous hydrogen production and copper removal from water, Int. J. Hydrog. Energy 36 (2011) 6538–6545.
[21] A. Benoit, I. Paramasivam, Y.-C. Nah, P. Roy, P. Schmuki, Decoration of TiO_2 nanotube layers with WO_3 nanocrystals for high-electrochromic activity, Electrochem. Commun. 11 (2009) 728–732.
[22] N.K. Shrestha, Y.-C. Nah, H. Tsuchiya, P. Schmuki, Self-organized nano-tubes of TiO_2–MoO_3 with enhanced electrochromic properties, Chem. Commun. (2009) 2008–2010.
[23] A. Ghicov, H. Tsuchiya, R. Hahn, J.M. Macak, A.G. Muñoz, P. Schmuki, TiO_2 nanotubes: H^+ insertion and strong electrochromic effects, Electrochem. Commun. 8 (2006) 528–532.
[24] Y.-C. Nah, A. Ghicov, D. Kim, S. Berger, P. Schmuki, TiO_2–WO_3 composite nanotubes by alloy anodization: growth and enhanced electrochromic properties, J. Am. Chem. Soc. 130 (2008) 16154–16155.
[25] S. Berger, A. Ghicov, Y.-C. Nah, P. Schmuki, Transparent TiO_2 nanotube electrodes via thin layer anodization: fabrication and use in electrochromic devices, Langmuir 25 (2009) 4841–4844.
[26] Q. Wang, Y.Z. Pan, S.S. Huang, S.T. Ren, P. Li, J.J. Li, Resistive and capacitive response of nitrogen-doped TiO_2 nanotubes film humidity sensor, Nanotechnology 22 (2011) 025501.
[27] Y. Zhang, W. Fu, H. Yang, Q. Qi, Y. Zeng, T. Zhang, R. Ge, G. Zou, Synthesis and characterization of TiO_2 nanotubes for humidity sensing, Appl. Surf. Sci. 254 (2008) 5545–5547.
[28] D. Fang, K. Huang, S. Liu, Z. Luo, X. Qing, Q. Zhang, High-density $NiTiO_3$/TiO_2 nanotubes synthesized through sol–gel method using well-ordered TiO_2 membranes as template, J. Alloy. Compd. 498 (2010) 37–41.
[29] S.Y. Heo, D.J. Kim, H. Jeon, B. Jung, Y.S. Kang, Vertically aligned anatase TiO_2 nanotubes on transparent conducting substrates using polycarbonate membranes, RSC Adv. 3 (2013) 13681–13684.
[30] S.J. Ku, G.C. Jo, C.H. Bak, S.M. Kim, Y.R. Shin, K.H. Kim, S.H. Kwon, J.-B. Kim, Highly ordered freestanding titanium oxide nanotube arrays using Si-containing block copolymer lithography and atomic layer deposition, Nanotechnology 24 (2013) 085301.
[31] T.R.B. Foong, Y. Shen, X. Hu, A. Sellinger, Template directed liquid ALD growth of TiO_2 nanotube arrays: properties and potential in photovoltaic devices, Adv. Funct. Mater. 20 (2010) 1390–1396.
[32] L.K. Tan, X. Liu, H. Gao, Vertically standing, highly ordered, and dimension and morphology controllable TiO_2 nanotube arrays via template-assisted atomic layer deposition, J. Mater. Chem. 21 (2011) 11084–11087.
[33] L. Cui, K.N. Hui, K.S. Hui, S.K. Lee, W. Zhou, Z.P. Wan, C.-N.H. Thuc, Facile microwave-assisted hydrothermal synthesis of TiO_2 nanotubes, Mater. Lett. 75 (2012) 175–178.
[34] B.D. Yao, Y.F. Chan, X.Y. Zhang, W.F. Zhang, Z.Y. Yang, N. Wang, Formation mechanism of TiO_2 nanotubes, Appl. Phys. Lett. 82 (2003) 281–283.
[35] J.-G. Chen, C.-Y. Chen, C.-G. Wu, C.-Y. Lin, Y.-H. Lai, C.-C. Wang, H.-W. Chen, R. Vittal, K.-C. Ho, An efficient flexible dye-sensitized solar cell with a photoanode consisting of TiO_2 nanoparticle-filled and SrO-coated TiO_2 nanotube arrays, J. Mater. Chem. 20 (2010) 7201–7207.
[36] D. Kuang, J. Brillet, P. Chen, M. Takata, S. Uchida, H. Miura, K. Sumioka, S.M. Zakeeruddin, M. Gra tzel, Application of highly ordered TiO_2 nanotube arrays in flexible dye-sensitized solar cells, ACS Nano 2 (2008) 1113–1116.
[37] H.-P. Jen, M.-H. Lin, L.-L. Li, H.-P. Wu, W.-K. Huang, P.-J. Cheng, E.W.-G. Diau, High-performance large-scale flexible dye-sensitized solar cells based on anodic TiO_2 nanotube arrays, ACS Appl. Mater. Interfaces 5 (2013) 10098–10104.
[38] Y.R. Smith, V. Subramanian, Heterostructural composites of TiO_2 mesh–TiO_2 nanoparticles photosensitized with CdS: a new flexible photoanode for solar cells, J. Phys. Chem. C 115 (2011) 8376–8385.
[39] Z. Liu, V. Subramania, M. Misra, Vertically oriented TiO_2 nanotube arrays grown on Ti meshes for flexible dye-sensitized solar cells, J. Phys. Chem. C 113 (2009) 14028–14033.
[40] J. Yu, D. Wang, Y. Huang, X. Fan, X. Tang, C. Gao, J. Li, D. Zou, K. Wu, A cylindrical core-shell-like TiO_2 nanotube array anode for flexible fiber-type dye-sensitized solar cells, Nanoscale Res. Lett. 6 (2011) 94.
[41] Y.-Y. Kuo, C.-H. Chien, Sinter-free transferring of anodized TiO_2 nanotube-array onto a flexible and transparent sheet for dye-sensitized solar cells, Electrochim. Acta 91 (2013) 337–343.
[42] S. Biswas, M. Shahjahan, Md.F. Hossain, T. Takahashi, Synthesis of thick TiO_2 nanotube arrays on transparent substrate by anodization technique, Electrochem. Commun. 12 (2010) 668–671.
[43] G.K. Mor, O.K. Varghese, M. Paulose, C.A. Grimes, Transparent highly ordered TiO_2 nanotube arrays via anodization of titanium thin films, Adv. Funct. Mater. 15 (2005) 1291–1296.
[44] G.K. Mor, K. Shankar, M. Paulose, O.K. Varghese, C.A. Grimes, Use of highly-ordered TiO_2 nanotube arrays in dye-sensitized solar cells, Nano Lett. 6 (2006) 215–218.
[45] J.Y. Kim, J.H. Noh, K. Zhu, A.F. Halverson, N.R. Neale, S. Park, K.S. Hong, A.J. Frank, General strategy for fabricating transparent TiO_2 nanotube arrays for dye-sensitized photoelectrodes: illumination geometry and transport properties, ACS Nano 5 (2011) 2647–2656.
[46] Y. Tang, J. Tao, Z. Dong, J.T. Oh, Z. Chen, The formation of micrometer-long TiO_2 nanotube arrays by anodization of titanium film on conducting glass substrate, Adv. Nat. Sci.: Nanosci. Nanotechnol. 2 (2011) 045002.
[47] K.N. Chappanda, Y.R. Smith, M. Misra, S.K. Mohanty, Site-specific and patterned growth of TiO_2 nanotube arrays from e-beam evaporated thin titanium film on Si wafer, Nanotechnology 23 (2012) 385601.
[48] J. Ni, C.J. Frandsen, K. Noh, G.W. Johnston, G. He, T. Tang, S. Jin, Fabrication of thin film TiO_2 nanotube arrays on Co–28Cr–6Mo alloy by anodization, Mater. Sci. Eng. C 33 (2013) 1460–1466.
[49] V. Galstyan, E. Comini, G. Faglia, A. Vomiero, L. Borgese, E. Bontempi, G. Sberveglieri, Fabrication and investigation of gas sensing properties of Nb-doped TiO_2 nanotubular arrays, Nanotechnology 23 (2012) 235706.

Biographies

Nam-Su Jang received the M.S. degree in nano fusion technology from the Pusan National University, Korea, in 2014. He is currently working toward the Ph.D. degree at the Pusan National University, Korea. His current research interests include synthesis and applications of functional nanomaterials, micromachined sensors and actuators, and flexbile/stretchable devices.

Min Seong Kim received the B.S. degree in nanomechatronics engineering from the Pusan National University, Korea, in 2014. He is currently working as a researcher at the Korea Advanced Institute of Science and Technology (KAIST), Korea. His current research interests include flexible electronics, human motion sensing, nano/micro manufacturing processes and system.

Soo-Hyung Kim received the Ph.D. degree in mechanical engineering from the University of Minnesota, USA, in 2003. In 2006, he joined the Pusan National University, where he is currently an Associate Professor of nanomechatronics engineering. His current research interests include synthesis and characterization of nanostructured materials, and their applications to the fields of photovoltaic and electronic devices.

Soo-Keun Lee is a principal researcher of the Nano/Bio Research Division at Daegu Gyeongbuk Institute of Science and Technology (DGIST) in Korea. Dr. Lee received his Ph.D. in applied sciences from Robert Gordon University (UK) in 2001, worked

as a research fellow and professor at the University of Strathclyde (UK) and POSTCH (Korea). He joined the DGIST in 2005. He is a multidisciplinary scientist with research interests in sensor development, environmental photocatalysis (nano-crystalline titania), and optoelectronics.

Jong-Man Kim received the Ph.D. degree in electrical engineering and computer science from the Seoul National University, Korea, in 2007. In 2008, he joined the Pusan National University, where he is currently an Associate Professor of nanomechatronics engineering. His current research interests include design, fabrication, and characterization of MEMS sensors and actuators, biomimetic engineering, synthesis and applications of functional nanomaterials, and flexbile/stretchable electronics.